Infrared-active phonons in carbon nanotubes

J.-L. Bantignies and J.-L. Sauvajol
Laboratoire des Colloïdes, Verres et Nanomatériaux (UMR CNRS 5587), CC 026, Université Montpellier II, 34095 Montpellier Cedex 5, France

A. Rahmani
Equipe de Physique Informatique et Modélisation des Systèmes, Université MY Ismail, Faculté des Sciences, BP 11201, Zitoune, 50000 Meknès, Morocco

E. Flahaut
Centre Interuniversitaire de Recherche et d'Ingénierie des Matériaux, (UMR CNRS 5085), Université Paul Sabatier, 31602 Toulouse Cedex 4, France

The aim of the present paper is to identify the main infrared vibrational features of carbon nanotubes. In this goal, infrared experiments have been performed on different well-characterized single-walled carbon nanotubes (SWCNTs) and double-walled carbon nanotubes (DWCNTs) as well as graphite and carbon aerogel. The comparison between the experimental spectra measured on these different samples allows us to identify the infrared-active modes of carbon nanotubes. In SWCNTs, the tangential modes are located around 1590 cm^{-1} and the radial mode around 860 cm^{-1}. This latter mode vanishes in the infrared spectrum of DWCNTs. Finally, in the infrared spectra of all the carbon nanotubes investigated, a band around 1200 cm^{-1} is evidenced and assigned to the *D*-band (disorder-induced band).

DOI: 10.1103/PhysRevB.74.195425 PACS number(s): 78.67.Ch, 78.30.Na

I. INTRODUCTION

Since the discovery of carbon nanotubes,[1] much attention has been devoted to the investigation of their vibrational properties, experimentally as well as theoretically. Resonant Raman scattering technique has been shown to provide a powerful tool for studying the phonon dynamic of single-walled carbon nanotubes (SWCNTs).[2,3] By contrast, the infrared-active modes of SWCNTs are very difficult to detect. Indeed, SWCNTs do not support a static dipole moment and the infrared (ir) activity is related to a dynamic dipole moment that is weak. Nevertheless, infrared spectroscopy has shown significant promise for the study of SWCNT chemistry.[4] Obviously, the use of ir spectroscopy to study the SWCNT chemistry implies the knowledge of the ir intrinsic vibrational modes of SWCNTs. The aim of the present investigation is to identify the intrinsic infrared features of carbon nanotubes.

Only few experiments have been devoted to the measurement of the infrared-active vibrational modes of SWCNTs.[5–9] Most of the observations and conclusions of these previous studies are sometimes opposite. For instance, two modes located around 873 and 1597 cm^{-1} have been reported in Ref. 6. These modes are upshifted with respect to the A_{2u} (868 cm^{-1}) and E_{1u} (1590 cm^{-1}) ir-active modes of graphite.[6,10] By contrast, in other investigations performed on functionalized SWCNTs[7] or industrially produced SWCNTs,[8] both ir-bands are downshifted by comparison to the related infrared-active modes in graphite. In Ref. 8, these bands are located around 820 and 1535 cm^{-1}, respectively. Very recently, an ir investigation was performed on thin films of SWCNT bundles. The sample used in this latter experiment was purifed (from successive oxydation processes) and vacuum annealed at 1400 °C.[4] The resulting sample was ultrasonicated in 2-propanol and several drops of the solution were deposited from solution onto ZnSe substrates for the ir experiments. By contrast with all the previous studies, a larger number of lines was observed in this latter investigation. The sharp lines in the ir spectra of these purified and annealed SWCNTs were assigned to one- and two-phonons modes.[9] Especially, eight distinct groups of lines located between 680 and 1600 cm^{-1} were assigned to first order ir modes belonging along A_2 and E_1 symmetry (see Table 1 in Ref. 9). In summary, a large disagreement is found in the literature concerning the assignment of the ir-active modes of SWCNTs. On the other hand, the infrared-active phonon modes of SWCNTs have been calculated from different methods: zone folding model,[11–13] tight binding approach,[14] force constant model,[15–18] and *ab initio* calculations.[19] Concerning the diameter dependence of the ir active modes these predictions are sometimes opposite.

The main aim of the present paper is to identify unambiguously the ir features of carbon nanotubes. In this goal, infrared experiments have been performed on different well-characterized single-walled (SWCNTs) and double-walled (DWCNTs) carbon nanotubes.

II. EXPERIMENT

Infrared experiments have been performed on graphite (sample 1), SWCNTs (samples 2–6), carbon aerogel (sample 7), and DWCNTs (sample 8). The SWCNT samples were prepared by the electric arc method[20] and laser ablation.[21] These samples were first characterized by x-ray diffraction. We have selected parts of the different samples that showed a strong intensity of the (10) Bragg peak. In consequence,

these parts contain a large amount of bundles (samples 2–5).[22] The main difference between the selected samples is the size of the bundles. Typically, the average number of tubes in a bundle is around 20 tubes in the SWCNT samples prepared by the electric arc method and above 50 tubes for the SWCNT samples prepared by laser ablation. On the other hand, we have also selected a part of a SWCNT sample prepared by the electric arc method that showed no (10) Bragg peak in its x-ray diffraction pattern (sample 6). By contrast with the other SWCNT samples (samples 2–4), x-ray diffraction has also revealed that this latter sample contained a significant amount of amorphous carbon. In all the samples, the tube diameters were estimated from the position of their radial breathing modes measured by Raman spectroscopy. The diameter distribution is centered around 1.4 nm (distribution width of about 0.2 nm). A DWCNT sample was prepared by the method described in Ref. 23. Transmission electronic microscopy (TEM) observations showed that DWCNTs are clean (no amorphous deposit) and generally isolated, or gathered into small-diameter bundles.[24] The outer (inner) diameters range from about 1.3 to 1.6 nm (from about 0.7 to 1 nm).[25] Carbon aerogels were prepared from the sol-gel polymerization of resorcinol with formaldehyde followed by CO_2 supercritical drying and carbonization (the method is described in Ref. 26). X-ray diffraction experiments have revealed the amorphous carbon character of this sample.

After outgassing and annealing all the samples at 230 °C for 24 h under dynamical vacuum, they were gently mixed with potassium bromide (KBr) and then pressed into pellets for infrared experiments.

Fourier transform infrared (FTIR) experiments was carried out on a Bruker IFS 113V spectrometer equipped with a N2-cooled MCT (mercury-cadnium telluride) detector. Transmission ir spectra were recorded in the 400–4000 cm^{-1} range. The spectral resolution was 2 cm^{-1} and 64 scans were coadded for each spectrum.

III. RESULTS

The 450–4000 cm^{-1} wave-number range of the ir transmission spectra measured on carbon aerogel (amorphous carbon), a SWCNT sample, and graphite are compared in Fig. 1. As expected, the intensities of the ir absorption bands are weak. Only small features centered around 860 and 1590 cm^{-1} are evidenced in graphite and SWCNTs. An additional component around 1190 cm^{-1} is observed in all the SWCNT samples (Fig. 2). It is the most intense band of the ir spectrum. No band in the stretching mode range of C═O (between 1600 and 1800 cm^{-1}), CH (2800–3000 cm^{-1}), and OH (3000–3600 cm^{-1}) groups was observed. Consequently, our SWCNT samples are free of usual functionalization. In carbon aerogel, bands around 880 cm^{-1}, 1590 cm^{-1}, and a very broad and complex feature centered around 1250 cm^{-1} are found.

In this paper, we focus on the identification of the main infrared modes of SWCNTs. In Fig. 2(a) (curves 2–6) the 800–900 cm^{-1} wave-number range of the ir spectra measured on five SWCNT samples are displayed. They are compared to the ir spectrum of graphite [Fig. 2(a), curve 1] and carbon aerogel [Fig. 2(a), curve 7]. In graphite, the weak (0.02% transmittance) and narrow band centered at 868 cm^{-1} was assigned to the A_{2u} out-of-plane vibration mode.[10] For all the SWCNT samples under consideration (samples 2–6), an ir band is systematically observed around 860 cm^{-1}. This band is assigned to the ir-active radial mode as predicted from calculations.[19] With respect to the position of the A_{2u} mode in graphite centered at 868 cm^{-1}, this band shows a downshift of 8 cm^{-1} in SWCNTs. Such a component is totally absent in the ir spectrum of the carbon aerogel in which a band at 880 cm^{-1} is observed [Fig. 2(a), curve 7]. Such a band was previously observed in amorphous carbon[27] confirming that carbon aerogel is an amorphous carbon sample as also revealed by x-ray diffraction (see the experimental section). A 880 cm^{-1} band is also found in the ir spectrum of the sample 6 [Fig. 2(a), curve 6] in agreement with the large amount of amorphous carbon present in this SWCNT sample (see the experimental section). Finally, in the SWCNT samples (samples 2–5) that show a clear bundle organization, the 880 cm^{-1} band is totally absent. Concerning the dependence of these radial modes with the tube diameters, in agreement with our results, *ab initio* calculations predict an upshift of the frequency of this mode with the diameter.[19]

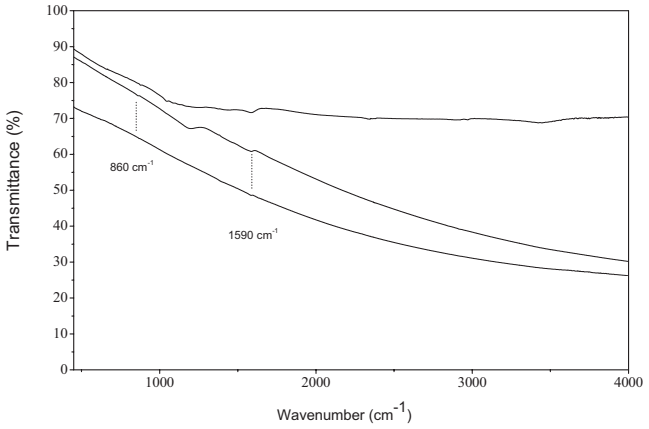

FIG. 1. The transmittance ir spectra of carbon aerogel (top), SWCNT sample (middle), and graphite (bottom). The spectra have been shifted for clarity.

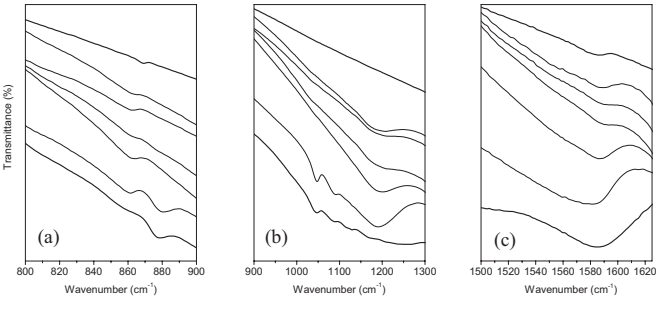

FIG. 2. Comparison between the transmittance ir spectra measured on several carbon materials. From top to bottom: graphite (curve 1), SWCNTs (curves 2–6), and carbon aerogel (curve 7). (a) The radial mode range, (b) the 900–1300 cm^{-1} range, and (c) the TM range. The spectra have been shifted for clarity.

The ir-active radial mode at 860 cm^{-1} does not show any significant sample dependence. Because the SWCNT samples under investigation mainly differ by the size of the bundles, we conclude, in agreement with recent calculations,[16] that the position of this infrared active mode does not significantly depend on the bundle size.

The wave-number range 900–1300 cm^{-1} is shown in Fig. 2(b). A broadband located around 1190 cm^{-1} is found in the ir spectrum of all the SWCNT samples [Fig. 2(b), curves 2–6]. This well-defined band is the most intense ir feature of the spectrum (Fig. 1). We come back on its attribution in the following. A very broad feature is observed around 1250 cm^{-1} in carbon aerogel [Fig. 2(b), curve 7]. In sample 6, other weak features (0.3% to 0.4 % transmittance) are found around 1045 and 1090 cm^{-1} [Fig. 2(b), curve 6]. Because these bands are also measured in carbon aerogel [Fig. 2(b), curve 7], they clearly originate from the ir response of the part of amorphous carbon present in sample 6. Additional weak lines (0.2% transmittance) are also observed around 1127, 1168 and 1188 cm^{-1} in carbon aerogel [Fig. 2(b)].

In the region of the tangential modes, the ir spectra of samples 2–5 show a broad band located around 1587 cm^{-1} [Fig. 2(c), curves 2–6]. In graphite, the E_{1u} in-plane vibration mode is located close of this same wave number [Fig. 2(c), curve 1]. In sample 6, this band is slightly downshifted to around 1582 cm^{-1} [Fig. 2(c), curve 6]. Finally, in carbon aerogel, a band is also observed around 1587 cm^{-1} [Fig. 2(c), curve 7]. This band displays a larger broadening than in graphite and SWCNTs. These results show that the position of the tangential mode does not significantly depend on the curvature of the graphene sheet and on the long range order. With regards to the large differencies between the structural parameters of the SWCNT samples investigated (bundles of different sizes), we conclude that the position of this band is not sensitive to the packing of the carbon nanotubes, in agreement with recent calculations.[16] With regards to the large width of this band and its nonsymmetric profile, a precise measurement of the position of this peak is not easy. In consequence, the wave number of this mode cannot be used as an efficient experimental tool to characterize the structure of SWCNT samples. Concerning the dependence of these tangential modes with the tube diameters, *ab initio* calculations predict an upshift of the frequency of this mode with the diameter. For diameter larger than 1.4 nm, the position of this band was more or less constant and close to that of graphene.[19] These latter predictions are in complete agreement with our data (see Table I).

In Fig. 3 are compared the ir spectra measured on SWCNT and DWCNT samples. The most important result is that the radial ir-mode located around 860 cm^{-1} in the SWCNT samples is silent in the DWCNT sample [Fig. 3(a)]. In the region of the tangential modes, a well- defined band located at 1580 cm^{-1} [Fig. 3(c)] is observed. The position of this band is located near those observed in the different carbon materials (graphite, SWCNT, and carbon aerogel). This observation agrees with our previous conclusion about the slight sensitivity of this mode to the structural organization of carbon nanotubes. Finally, a well-defined band at 1190 cm^{-1} is also found in the ir spectrum of this well-characterized DWCNT sample [Fig. 2(b)]

TABLE I. ir frequencies for our data and those given in the literature; w, m, b, and s stand for weak, middle, broad, and strong intensity, respectively.

Expt. ν (cm^{-1})	Attribution	References	Material
682 (w)	1st order A_2	9	Purified SWCNT
806 (w)	1st order A_2	9	
854 (w)	1st order E_1	9	
820 (w)		7,8	Purified SWCNT
840 (w)		7,8	Purified SWCNT
860 (w)	radial mode	This work	SWCNT
868 (w)	A_{2u}	6,19	Graphite
873 (w)		6	SWCNT
880 (w)	1st order A_2	9	Purified SWCNT
1045		This work	Amorphous carbon
1090		This work	Amorphous carbon
1127		This work	Amorphous carbon
1168		This work	Amorphous carbon
1188		This work	Amorphous carbon
1190 (b,s)	D-band	This work	SWCNT
1250 (b,s)		This work	Amorphous carbon
1262	1st order A_2	9	Purified SWCNT
1369	1st order A_2	9	Purified SWCNT
1535		8	Purified SWCNT
1541	1st order A_2	9	Purified SWCNT
1555		8	Purified SWCNT
1564	1st order E_1	7,9	Purified SWCNT
1580		This work	DWCNT
1582 (m)	Tangential mode	This work	
1585	1st order E_1	9	Purified SWCNT
1587 (m)	Tangential mode	This work	SWCNT
1587 (m)		This work	Amorphous carbon
1590 (m)	E_{1u}	6,19	Graphite
1597 (m)		6	SWCNT

IV. DISCUSSION

These results question the assignments of the ir features of a SWCNT previously proposed.[6–8] Clearly, our data and the *ab initio* calculations are opposite to the results of Kulh-

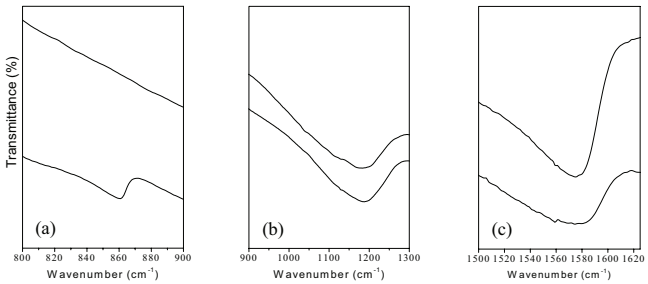

FIG. 3. Comparison between the transmittance ir spectra measured on a DWCNT sample (top) and a SWCNT sample (bottom). (a) The radial mode range, (b) the 900–1300 cm^{-1} range, and (c) the TM range. The spectra have been shifted for clarity.

mann *et al.* who assign the ir-active radial mode to the experimental line located around 874 cm^{-1} and the tangential modes to the line located at 1600 cm^{-1}. Both lines are upshifted with respect to the A_{2u} mode and E_{1u} infrared-active modes in graphite centered at 868 and 1590 cm^{-1}, respectively. In other investigations,[7,8] significant downshifts of the ir-active radial mode (lines located around 820 and 840 cm^{-1}) and tangential modes (lines around 1535, 1555, and 1564 cm^{-1}[17]) are found. The experimental downshift of radial and tangential modes when the diameter increases[8] is opposite to the predictions of the *ab initio* calculations.[19] It must be emphasized that these latter investigations have been performed on purified samples. Because functionalization of the tubes usually occurs under purification treatments, a part of the shift can be mainly assigned to the effect of the functionalization on the vibrational modes (extrinsic effects) and consequently they do not reflect the intrinsic phonon dynamics of SWCNTs.

Clearly, the radial ir-active mode observed around 860 cm^{-1} in a SWCNT is not observed in a DWCNT. The possible balancing between the dynamic dipole moments on the inner and outer nanotubes can lead to the vanishing of the collective radial mode of both layers in a DWCNT. *Ab initio* calculations of the ir spectrum of a DWCNT in the framework of the density functional theory are in progress to confirm this assumption.

The observation of a component around a 1190 cm^{-1} in all the carbon nanotube samples investigated suggests that this band is an infrared feature of carbon nanotubes. An ir-active mode is predicted in this frequency range (more precisely, in the 1200–1250 cm^{-1} range in most of the modelizations). However, its intensity is expected to be weak with regards to the intensity of the main infrared modes in SWCNTs.[16] On the other hand, in the Raman spectrum of the same SWCNT samples, a *D*-band is observed. In Raman scattering, the *D*-band is activated by the presence of defects which lower the crystalline symmetry of the quasi-infinite lattice. As expected in the framework of a double-resonance process,[28,29] the position of this band is excitation dependent. With regards to the linear dependence of the position of the *D*-band with the laser energy (E_{Laser}),[30] its position is predicted around 1200 cm^{-1} at $E_{Laser}=0$. In consequence, considering the symmetry-breaking in SWCNTs containing structural defects, such a *D*-band can be active in the ir spectrum, and its frequency is expected around 1200 cm^{-1}. On the basis of this information, we assign the 1190 cm^{-1} feature observed in all the carbon nanotubes as resulting from the overlap between a weak ir-active mode of a SWCNT and a strong contribution of the *D*-band.

Finally, the observation of few ir-active modes in the range 600–1800 cm^{-1} is in complete disagreement with the great number of weak and sharp ir modes reported in the most recent ir investigation (Figs. 1 and 2 and Table 1 in Ref. 9). It must be emphasized that to prepare the films used in this latter experiment, successive oxydation processes, vacuum annealing, and an ultrasonication process were performed.[9] Clearly, our ir spectra measured on different well-characterized samples, with no chemical and sonication treatments, are opposite to these observations. Some of the lines attributed to first order ir modes in Ref. 9 could be assigned to defect modes created by the successive treatments. Especially, because the sample was ultrasonicated after the purification treatment and before the ir experiments, it is possible that a significant amount of short tubes was obtained during this latter operation leading to the observation of a great number of lines as predicted by recent calculations.[16]

V. CONCLUSION

In conclusion, the experimental infrared spectra measured on well-characterized different samples allow us to identify unambiguously the ir fingerprints of a SWCNT. The radial mode and tangential modes are unambiguously identified around 860 and 1587 cm^{-1}, respectively. With regards to the radial displacements of the carbon atoms involved in the radial mode located around 860 cm^{-1} in a SWCNT, its frequency is sensitive on the curvature of the tubes and on the interaction between tubes as revealed by its nonactivity in a DWCNT. Comparisons with previous investigations suggest that the frequencies of both modes depend on extrinsic effects (for instance, the functionalization of the nanotube), which affect the dynamics of the phonon. In all the carbon nanotubes, a band located around 1200 cm^{-1} is evidenced. It mainly origins from the contribution of the *D*-band to the ir spectrum of SWCNTs with defects.

ACKNOWLEDGMENT

This work was supported by a CNRS-France/CNRST-Morocco agreement.

[1] S. Iijima, Nature (London) **354**, 56 (1991).
[2] M. S. Dresselhaus and P. C. Eklund, Adv. Phys. **49**, 705 (2000), and references therein.
[3] S. Reich, C. Thomsen, and J. Maultzsch: *Carbon Nanotubes. Basic Concepts and Physical Properties* (Wiley-VCH, Weinheim, Germany, 2004).
[4] U. J. Kim, C. A. Furtado, X. Liu, G. Chen, and P. C. Eklund, J. Am. Chem. Soc. **127**, 15437 (2005).
[5] S. Curran, D. Weldon, W. Blau, H. Zandbergen, J. Kastner, and H. Kuzmany, Fullerenes Photon. **2284**, 33 (1994).
[6] U. Kuhlmann, H. Jantoljak, N. Pfander, P. Bernier, C. Journet, and C. Thomsen, Chem. Phys. Lett. **294**, 237 (1998).
[7] J. Zhang, H. Zou, Q. Qing, Y. Yang, Q. Li, Z. Liu, X. Guo, and Z. Du, J. Phys. Chem. B **107**, 3712 (2003).
[8] C. Branca, F. Frusteri, V. Magazu, and A. Mangione, J. Phys. Chem. B **108**, 3469 (2004).
[9] U. J. Kim, X. M. Liu, C. A. Furtado, G. Chen, R. Saito, J. Jiang, M. S. Dresselhaus, and P. C. Eklund, Phys. Rev. Lett. **95**,

157402 (2005).
[10] R. J. Nemanich, G. Lucovski, and S. A. Solin, Solid State Commun. **23**, 117 (1977).
[11] R. A. Jishi, L. ven Kataraman, M. S. Dresselhaus, and G. Dresselhaus, Chem. Phys. Lett. **209**, 77 (1993).
[12] P. C. Eklund, J. M. Holden, and R. A. Jishi, Carbon **33**, 959 (1995).
[13] R. Saito, T. Takeya, T. Kimura, G. Dresselhaus, and M. S. Dresselhaus, Phys. Rev. B **57**, 4145 (1998).
[14] D. Kahn and Jian Ping Lu, Phys. Rev. B **60**, 6535 (1999).
[15] V. N. Popov, V. E. Van Doren, and M. Balkanski, Phys. Rev. B **59**, 8355 1999; **61**, 3078 (2000).
[16] K. Sbai, A. Rahmani, H. Chadli, J.-L. Bantignies, P. Hermet, and J.-L. Sauvajol (unpublished).
[17] M. Damnjanović, I. Milosević, T. Vuković, and R. Sredenović, Phys. Rev. B **60**, 2728 (1999).
[18] E. Dobardzić, I. Milosević, B. Nikolić, T. Vuković, and M. Damnjanović, Phys. Rev. B **68**, 045408 (2003).
[19] O. Dubay and G. Kresse, Phys. Rev. B **67**, 035401 (2003).
[20] C. Journet, W. K. Maser, P. Bernier, A. Loiseau, M. L. de la Chapelle, S. Lefrant, P. Deniard, R. Lee, and J. E. Fisher, Nature (London) **388**, 756 (1997).
[21] T. Guo, P. Nikolaev, A. Thess, D. T. Colbert, and R. E. Smalley, Chem. Phys. Lett. **243**, 49 (1995).
[22] S. Rols, E. Anglaret, L. Henrard, R. Almairac, and J.-L. Sauvajol, Eur. Phys. J. B **10**, 263 (1999).
[23] E. Flahaut, R. Bacsa, A. Peigney, and Ch. Laurent, Chem. Commun. (Cambridge) **10**, 1442 (2003).
[24] J.-F. Colomer, L. Henrard, E. Flahaut, G. Van Tendeloo, A. A. Lucas, and Ph. Lambin, Nano Lett. **3**, 685 (2003).
[25] J. Cambedouzou, J. L Sauvajol, A. Rahmani, E. Flahaut, A. Peigney, and C. Laurent, Phys. Rev. B **69**, 235422 (2004).
[26] C. Lin and J. A. Ritter, Carbon **35**, 1271 (1997).
[27] J. Kuhn, R. Brabdt, H. Mehling, R. Petricević, and J. Fricke, Interface (USA) **225**, 58 (1998).
[28] C. Thomsen and S. Reich, Phys. Rev. Lett. **85**, 5214 (2000).
[29] R. Saito, A. Jorio, A. G. Souza Filho, G. Dresselhaus, M. S. Dresselhaus, and M. A. Pimenta, Phys. Rev. Lett. **88**, 027401 (2001).
[30] S. D. M. Brown, A. Jorio, M. S. Dresselhaus, and G. Dresselhaus, Phys. Rev. B **64**, 073403 (2001).